Identify Influential Spreaders in Asymmetrically Interacting Multiplex Networks

Ying Liu, Qi Zeng, Liming Pan, and Ming Tang

***Abstract*—Identifying the most influential spreaders is crucial to use limited resource to control spreading in the network. Existing studies of ranking node importance in multilayer networks are mostly based on the network structure, while neglecting how the structural and dynamical couplings of multiple layers impact the spreading influence of nodes in coevolving dynamics. Here we investigate on the identification of influential spreaders in the information-disease coupled spreading dynamics on multiplex networks. Firstly we explicitly reveal that three interlayer coupling factors, which are the two-layer relative spreading rate, the interlayer coupling strength and the interlayer degree correlation, significantly impact the spreading influence of a node in the contact layer where disease spreads. The suppression effect from the information layer makes the structural centrality of nodes in the contact layer fail to predict their influence. Then by mapping the coevolving spreading processes into percolation and using the message-passing approach, we propose a method to calculate the outbreak size of disease starting from a single seed node, which is used to estimate the spreading influence of the node and identify the most influential spreaders in coevolving dynamics on multiplex networks. Our work gives a feasible framework to investigate critical nodes in multiplex networks.**

***Index Terms*—Multiplex network, influential spreader, asymmetrically interacting dynamics, centrality measure.**

I. Introduction

MANY activities in society can be described as spreading processes on networks, such as the spreading of epidemic disease through contacts between human beings, information dissemination through emails and mobile phones of individuals, and the diffusion of ideas among friends and community members. Identifying the most influential spreaders is an important step to control the spreading processes, e.g. to hinder epidemic outbreaks [1], conduct successful advertisements for new products [2] and protect key members in ecosystems [3]. A commonly accepted way to rank and identify important nodes in a network is to use the centrality measures, such as degree, betweenness [4], eigenvector centrality [5], PageRank [6], non-backtracking centrality [7], and k-shell index [8]. Based on the idea of centrality, there are a lot of achievements in the identification of important nodes in single layer networks [9], [10], [11], [12], [13], [14], which help us to better understand the network structure and function.

In the real-world, from city infrastructure to human interactions, many complex systems are interconnected and are better described by the multilayer network [15]. For example, the air transportation network can be described as a multilayer network where nodes represent airports and each commercial airline corresponds to a different layer [16]. In social networks, individuals interact in different ways like being friends, colleagues, schoolmates, or interacting on different online social platforms [17], where each type of connections is represented by a layer. The multiplex network is a particular type of multilayer network, in which a set of nodes represent the same individuals in all layers, and their edges in different layers represent various friendship patterns, such as the social networks.

It is thus natural to use the multilayer formalism to study the scenarios where different dynamical processes interplay, such as the cooperative contagion processes spreading in a host population [18], and the competitive epidemic spreading or opinion spreading on multilayer networks [19], [20], [21]. A special case attracting much attention is the information-disease asymmetrically interacting processes [22], [23]. When an epidemic disease outbreaks in a district, the information on it is swiftly transmitted through the online social media, telephone, mass media, et al. The spreading of information suppresses the disease spreading because of the awareness people arise after receiving the information [24], and the spreading of disease promotes the diffusion of information, which are two asymmetrically interacting processes.

While many real-world complex systems can be modeled as multilayer networks, neglecting the multiple relationships between nodes or simply aggregating them into a single network alters the structural and dynamical properties of the system, leading to inaccurate identification of important nodes [25], [26]. In recent years, there are some progresses in identifying the critical nodes in multilayer networks [27], [28], [29], and

Manuscript received 24 July 2022; revised 30 January 2023; accepted 5 February 2023. Date of publication 14 February 2023; date of current version 16 June 2023. This work was supported in part by the National Natural Science Foundation of China under Grants 12231012, 61802321,11975099, 62006122, and 82161148012, in part by Sichuan Science and Technology Program under Grant 2020YJ0125, and in part by the Science and Technology Commission of Shanghai Municipality under Grant 22DZ2229004. Recommended for acceptance by Filippo Radicchi. *(Corresponding authors: Ying Liu; Ming Tang.)*

Ying Liu is with the School of Computer Science, Southwest Petroleum University, Chengdu 610500, China, and also with the Big Data Research Center, University of Electronic Science and Technology of China, Chengdu 611731, China (e-mail: shinningliu@163.com).

Qi Zeng is with the School of Computer Science, Southwest Petroleum University, Chengdu 610500, China (e-mail: swpu_zengqi@163.com).

Liming Pan is with the School of Computer and Electronic Information, Nanjing Normal University, Nanjing 210023, China (e-mail: pan.liming@njnu.edu.cn).

Ming Tang is with the School of Physics and Electronic Science, East China Normal University, Shanghai 200241, China, and also with the Shanghai Key Laboratory of Multidimensional Information Processing, East China Normal University, Shanghai 200241, China (e-mail: tangminghan007@gmail.com).

Digital Object Identifier 10.1109/TNSE.2023.3243560

the centrality measures are extended from single layer network to multilayer network which focus on the multilayer structure. Examples are the Multiplex PageRank and eigenvector-based centrality in multiplex network. But how the interplay between the multiple processes on the multilayer network impacts the functional influence of nodes is still unknown, and new ranking methods considering the structural and dynamical interplay between layers are still lacking.

In modern times, the epidemics spread more easily due to the growing transportation infrastructures [30]. Such as the ongoing coronavirus disease 2019 (COVID-19) quickly sweeps around the world and causes enormous economic loss in a short time. Timely and accurately identifying the influential spreaders is of great importance to efficiently suppress epidemics [31]. In this manuscript, based on an asymmetrically interacting information-disease spreading model on multiplex network, we work on explicitly revealing how the structural and dynamical coupling factors of multiple layers impact the spreading influence of nodes, and then step further to propose a new method to rank and identify influential spreaders in the multiplex networks. In our study, the multiplex network consists of two layers. The upper layer is a communication network on which information spreads, and the lower layer is a physical contact network representing social contacts between individuals and on which disease transmits. The spreading of information suppresses the spreading of disease, while the spreading of disease promotes the information diffusion, which are two asymmetrically interacting processes. As in real applications controlling the spreading of disease is usually the fundamental purpose, we concentrate on the influence of nodes in disease spreading.

Firstly, we study on how the two-layer coupling factors impact the degree and eigenvector centrality on the physical contact layer to predict the spreading influence of nodes in the coevolving dynamics. Discovering the performance of centralities under different values of structural and dynamical coupling parameters is meaningful. Due to the difficulty in collecting network data, when we only have the network data of contact layer, we can evaluate how accurately the centrality can predict the influential spreaders.

Secondly we propose an effective framework to rank the node influence in the asymmetrically interacting multiplex networks. Specifically speaking, by mapping the coevolving spreading dynamics into bond percolation and using the message-passing approach, we calculate the spreading outbreak size for each node as the seed, which can be used to rank the influence of disease spreaders in the multiplex network. The accurate identification of disease spreaders is very important in real-world epidemic control.

To the best of our knowledge, this work is the first step in explicitly revealing how the two-layer coupling factors impact the spreading influence and the performance of centralities in identifying influential spreaders. Our main contributions in this paper are as follows:

- We discover how three coupling factors, which are the relative spreading rate of the two layers, the coupling strength and the interlayer degree correlation, impact the accuracy of centrality measures in predicting spreading influence in multiplex networks.
- By mapping the coevolving spreading dynamics into percolation, we propose a method to accurately rank the spreading influence of nodes.
- We numerically evaluate our proposed method in multiplex networks and show its superiority over the benchmark centralities in identifying influential spreaders.

The rest of the paper is organized as follows. In Section II, we briefly introduce related works. In Section III, the information-disease spreading model on multiplex network is described. In Section IV, we demonstrate the impact of interlayer coupling factors on the accuracy of centralities in identifying influential spreaders. In Section V, we map the coevolving spreading dynamics into percolation and propose a new method for ranking the spreading influence of nodes. In Section VI, we compare the efficacy of different metrics on both synthetic and real-world multiplex networks. Finally in Section VII, we give the conclusion.

II. Related Works

To identify the most important nodes in the multilayer networks, a lot of centrality measures are proposed, which are in general extended from centralities in single networks. For example, the Multiplex PageRank is a natural extension of PageRank in multiplex network, which considers that the centrality of a node in one network is affected by the centrality of the node in another layer [32]. A Functional Multiple PageRank is defined on the weight of multilinks (connections in different layers) where the link overlap between layers is considered [33]. The eigenvector centrality in multiplex networks takes into account the mutual influence of layers [34], and a supracentrality matrix which couples the centrality matrices of the individual layers is used [35]. The tensor framework mathematically describes the intralayer and interlayer relationships [36], and tensor decomposition is then used to identify critical nodes [37]. In the tensorial formalism, Domenico et al. generalize the eigenvector centrality, PageRank and betweenness centrality to multilayer network and define the versatility to identify the most important nodes [38]. A family of multilayer PCI (Power Community Index) measures generalized from h-index consider the density of a node's intra and inter connections and can be computed from the local structure of the network [39].

Although there are such progresses in identifying critical nodes on multilayer networks, most of them are based on the structure of the network, while neglecting how the structural and dynamical couplings between multiple layers influence the dynamical importance of nodes in the network. In a multilayer network, the interplay between the network structure and spreading dynamics on top of it largely influences the role of nodes in the network [40]. Identifying the critical nodes must take both the structural and dynamical characteristics of the network into consideration. In a study, the authors synthesized the centrality of nodes in both layers and the dynamical parameters to form a measure to quantify the node influence in symmetrically interacting interconnected networks, and the results showed that taking both layers' structure and dynamical parameters into consideration led to a better ranking result of the critical nodes [41]. But how the coevolving dynamics impacts

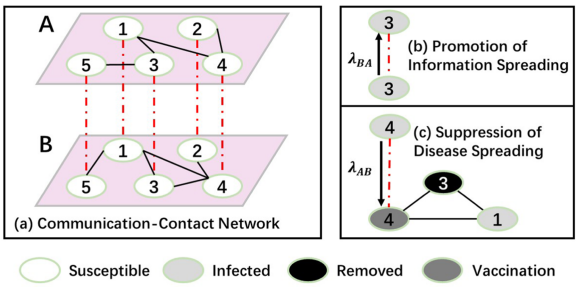

Fig. 1. The information-disease spreading processes on a communication-contact multiplex network. (a) The multiplex network consists of a communication layer A with SIR dynamics and a physical contact layer B with SIRV dynamics. (b) An infected node in layer B promotes the information spreading by changing its counterpart into informed state at rate λ_{BA}. (c) An informed node in layer A suppresses the disease spreading by changing its counterpart into vaccinated state at rate λ_{AB}.

on the spreading influence of nodes is unknown, and new ranking methods that considering the structural and dynamical interplay between layers are still lacking.

III. The Information-Disease Spreading Model on Multiplex Network

We use an asymmetrically interacting model [42] to describe the coevolving dynamics of disease and information spreading on multiplex network as shown in Fig. 1. Consider a multiplex network consisting of two layers. The upper layer represents the information communication network labeled as layer A and the bottom layer represents the physical contact network labeled as layer B. In the communication layer (layer A), the classical susceptible-infected-recovered (SIR) model is used to describe the spreading of information on disease. In the SIR model, node can be in one of the three states: (1) susceptible (S), in which the individual has not received any information about the disease, (2) infected (or informed for information transmission, I), in which the individual is aware of the disease and is able to transmit the information, or (3) recovered (R) in which the individual has received the information but is not willing to transmit the information to others. The informed node tries to transmit information to its neighbors at rate β_A. The informed node recovers at rate μ_A in the next time step. Once a node becomes recovered, it will remain in the state in the subsequent time steps.

The spreading of disease on the physical contact layer B is described by the SIRV model [43], where a vaccinated (V) state is introduced. A vaccinated node will not be infected by any node. The SIR dynamics is the same as layer A, with the infection rate and recovery rate denoted as β_B and μ_B respectively. The dynamical coupling of the two layers is as follows. For an informed individual in layer A, if its counterpart in layer B is susceptible, then the counterpart node changes to vaccinated state at rate λ_{AB}. The parameter λ_{AB} ranges in [0,1] and represents the extent to which people take care of the information and are willing to take vaccination. For a susceptible node in layer B, if its counterpart in layer A is in susceptible state, then in the next time step it may become either vaccinated at rate λ_{AB} if its counterpart in layer A is getting informed or infected by its infected neighbors in layer B. In this case, vaccination and infection will compete for the chance to affect such susceptible node in layer B. Take p_A and p_B as the probability that the vaccination or infection wins respectively, then

$$p_A = \frac{1-(1-\beta_A)^{n_i^A}}{\left[1-(1-\beta_A)^{n_i^A}\right]+\left[1-(1-\beta_B)^{n_i^B}\right]} \quad (1)$$

and

$$p_B = \frac{1-(1-\beta_B)^{n_i^B}}{\left[1-(1-\beta_A)^{n_i^A}\right]+\left[1-(1-\beta_B)^{n_i^B}\right]}, \quad (2)$$

where n_i^A is the number of informed neighbors of the counterpart node in layer A, and n_i^B is the number of infected neighbors of the considered node in layer B. If vaccination wins out, the node in layer A is informed with probability $1-(1-\beta_A)^{n_i^A}$ and then the couterpart node in layer B is vaccinated at rate λ_{AB}. Else, if the infection wins out, the node is infected in layer B with probability $1-(1-\beta_B)^{n_i^B}$ and its counterpart node changes to the informed state at rate λ_{BA}, which ranges in [0,1]. This represents the extent to which an infected individual is aware of and willing to transmit the information of the epidemic disease. A summary of the parameters used in the spreading model is demonstrated in Table I.

TABLE I
Parameters Used in the Spreading Model

Parameter	Description
β_A	information transmission rate
β_B	disease transmission rate
μ_A	information recovery rate
μ_B	disease recovery rate
λ_{AB}	vaccination rate
λ_{BA}	informing rate

IV. Revealing the Impact of Interlayer Coupling Factors

It is pointed out that the asymmetrically interacting dynamics will alter the activities of nodes on the multiplex networks [22]. Now we study on how three dynamical and structural coupling factors, which are the relative spreading rate of the two layers, the dynamical coupling strength and the interlayer degree correlation, affect the spreading influence of nodes and thus change the accuracy of centrality in predicting nodes' influence in the physical contact layer, which is our focus. The relative spreading rate of the two layers is defined as

$$\gamma_{AB}^{\lambda} = \lambda_A/\lambda_B, \quad (3)$$

where $\lambda_A = \beta_A/\mu_A$ and $\lambda_B = \beta_B/\mu_B$ are the effective transmission rate in layer A and B respectively. For simplicity, we set $\mu_A = \mu_B = 1$. The dynamical coupling strength of the two layers is represented by the two parameters λ_{AB} and λ_{BA}, which are the vaccination rate and informing rate respectively. The interlayer degree correlation m_s is quantified by the Spearman

rank correlation coefficient, which is defined as

$$m_s = 1 - 6\frac{\sum_{i=1}^{N}\Delta_i^2}{N(N^2-1)}, \tag{4}$$

where N is the network size and Δ_i is the rank difference of node i in the degree sorting list of each layer. m_s ranges in $[-1, 1]$. In our numerical simulations, different values of interlayer degree correlation are used. We tune the interlayer degree correlation in this way: Firstly we generate the degree sequence of layer A, and copy this sequence for nodes in layer B. Then we randomly exchange the degrees of any pair of nodes in layer B until the desired interlayer degree correlation is reached. We use positive degree correlations in simulations. This is because many real-world networks are positively correlated. Furthermore, in the asymmetrical coevolving dynamics, a negative correlation makes one layer have relatively small impact on the other layer [44].

A. Construct the Multiplex Network

In simulations, we use the uncorrelated configuration model (UCM) to generate each layer of the multiplex network, which follows a power law degree distribution $p(k) \sim k^{-\gamma}$. We first construct layer A with $N = 10000$, the power exponent $\gamma = 2.6$, and average degree $< k >= 6$. The minimal degree $k_{min} = 3$, and the maximal degree $k_{max} = \sqrt{N}$. Then we copy the nodes and their degrees of layer A, randomly exchange degrees of nodes and generate the edges to form layer B. Each node in layer A has a counterpart in layer B. At the beginning of the interacting dynamical processes, all nodes are set to be susceptible in both layers except the seed node. The seed node is infected in layer B and its counterpart in layer A is informed, which will initiate the disease spreading on layer B and information spreading on layer A respectively. The spreading processes stop until on both layers there is no infected or informed node. We record the final fraction of recovered nodes in layer B as the real spreading influence of the seed node, which is averaged over 100 independent realizations.

B. The Benchmark Centralities

Suppose an undirected network represented as G(V, E), where $V = \{v_1, v_2, \ldots, v_n\}$ is the set of nodes and $E = \{e_1, e_2, \ldots, e_m\}$ is the set of edges. The adjacency matrix of the graph G is $A_{n*n} = a_{ij}$, where $a_{ij} = 1$ means there is an edge between nodes i and j, otherwise $a_{ij} = 0$. The degree $k_i = \sum_1^n a_{ij}$ of node i is defined as the number of its direct neighbors, which is a simple but effective way to quantify the potential influence of nodes in the network. The larger the degree, the more neighbors the node is able to influence directly. The time complexity of calculating degree is $O(N)$, where N is the size of the network.

The idea of eigenvector centrality is that not all neighbors are equivalent. The node is important if it connects to many neighbors which are themselves important. The eigenvector centrality of node i is defined as

$$e_i = \lambda^{-1}\sum_{n=1}^{N} a_{ij}e_j, \tag{5}$$

where λ is the largest eigenvalue of the adjacency matrix A, $e = \{e_1, e_2, \ldots, e_n\}^T$ is the eigenvector of matrix A corresponding to the largest eigenvalue λ. If writing in the form of matrix, then it is $\lambda e = Ae$. In our work, the degree and eigenvector centrality of nodes in layer B are used as benchmark methods to identify the most influential nodes in disease spreading.

The collective influence (CI) [9] of a node at level l is defined as

$$CI_l(i) = (k_i - 1)\Sigma_{j\in\partial Ball(i,l)}(k_j - 1), \tag{6}$$

where k_i is the degree of node i, $Ball(i, l)$ is the node set inside a ball of radius l (the shortest path) around node i, and $\partial Ball(i, l)$ is the frontier of the ball, i.e., the nodes at distance l from i. The CI can identify those low-degree nodes surrounded by hierarchical coronas of hubs as optimal influencers and is proved to have better performance than other heuristic rankings to identify influential nodes in networks. In this paper, we use $l = 2$ to calculate the CI of nodes.

The idea of non-backtracking (NB) centrality [7] is similar to that of the eigenvector centrality, but avoids the problem of localization on hub nodes. The NB centrality is calculated by using the Hashimoto or non-backtracking matrix $\mathbf{B}$, which is defined as

$$x_j = \sum_i A_{ij}\nu_{i\to j}, \tag{7}$$

where A_{ij} is the adjacency matrix of the network, $\nu_{i\to j}$ is the element of the leading eigenvector of the non-backtracking matrix $\mathbf{B}$ of the network.

C. Evaluation Methods

We use the Kendall's tau correlation coefficient [45] and the imprecision function [8] to quantify how accurately the considered measure can predict the disease-spreading influence of nodes in the asymmetrically interacting processes on multiplex networks. The Kendall's tau correlation coefficient quantifies the consistency of two ranking lists for a set of objects. It is defined as

$$\tau = \frac{\sum_{i<j} sgn[(x_i - x_j)(y_i - y_j)]}{\frac{1}{2}n(n-1)}, \tag{8}$$

where sgn(x) is a sign function, which returns 1 if $x > 0$, -1 if $x < 0$, and 0 if $x = 0$. n is the number of nodes in the lists. x_i and x_j are the rank of nodes i and j in ranking list 1, while y_i and y_j are the rank of nodes i and j in ranking list 2. If the node pair i and j has a concordant order in ranking lists 1 and 2, $(x_i - x_j)(y_i - y_j) > 0$. If the node pair i and j has a discordant order in ranking lists 1 and 2, $(x_i - x_j)(y_i - y_j) < 0$. If the nodes i and j have an identical rank in either list 1 or list 2, $(x_i - x_j)(y_i - y_j) = 0$. In our applications, nodes are ranked by centrality measure in ranking list 1 and are ranked by their real spreading influence in ranking list 2. A large correlation coefficient τ implies that the centrality can better predict the spreading influence of nodes.

The imprecision function is defined as

$$\varepsilon(p) = 1 - \frac{M(p)}{M_{eff}(p)}, \tag{9}$$

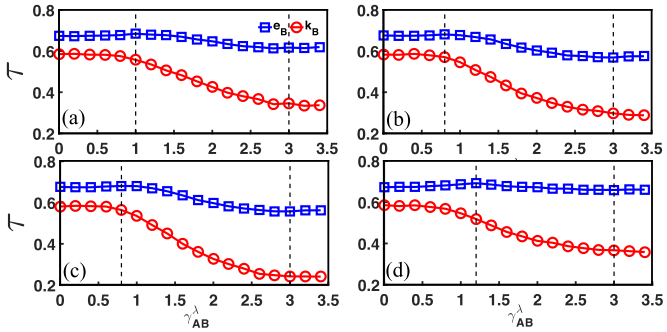

Fig. 2. Dependence of the Kendall's tau correlation of the eigenvector centrality and degree with the real spreading influence of nodes on the two-layer relative spreading rate. With the increase of γ^{λ}_{AB}, τ_{e_B} and τ_{k_B} first remain stable and then decrease obviously. τ_{e_B} and τ_{k_B} become stable again when γ^{λ}_{AB} exceeds 3.0. Other parameters are set as (a) $\lambda_{AB} = 0.7, \lambda_{BA} = 0.1, m_s = 0.5$, (b) $\lambda_{AB} = 1.0$, $\lambda_{BA} = 0.1$, $m_s = 0.5$, (c) $\lambda_{AB} = 1.0$, $\lambda_{BA} = 0.1$, $m_s = 0.7$ and (d) $\lambda_{AB} = 1.0, \lambda_{BA} = 0.3, m_s = 0.5$.

where p is the fraction of the network size N ($p \in [0, 1]$). $M(p)$ is the average spreading influence of pN nodes with the highest centrality, and $M_{eff}(p)$ is the average spreading influence of pN nodes with the highest spreading influence. This function quantifies how close to the optimal spreading is the average spreading of the pN nodes with the highest centrality. The smaller the ε value, the more accurate the centrality is a measure to identify the most influential spreaders.

D. Results

Firstly, we study on the impact of two-layer relative spreading rate on the accuracy of centrality in layer B. The accuracy of centrality in predicting node influence is quantified by the Kendall's tau correlation of the centrality and spreading influence as shown in Fig. 2. To concentrate on the relative spreading rate γ^{λ}_{AB}, we fix other coupling parameters and demonstrate the results. The impact of those parameters when they vary are discussed later. At $\gamma^{\lambda}_{AB} = 0$, it corresponds to the case when there is only disease spreading on layer B. The change of correlation τ is due to the change of spreading influence of nodes, which is suppressed by information spreading in layer A.

It can be seen from Fig. 2 that τ decreases with increasing γ^{λ}_{AB}. In Fig. 2(a) when $\gamma^{\lambda}_{AB} < 1.0$, the τ_{e_B} and τ_{k_B} are relatively stable. This means when the information spreads slowly, or even slower than the disease, it has little impact on disease spreading. When γ^{λ}_{AB} increases to the range [1.0, 3.0], τ_{e_B} and τ_{k_B} largely decrease. This is because when the information spreads faster than the disease, more nodes in layer B will be vaccinated. The spreading influence of nodes in layer B is suppressed by the information spreading. The faster the information spreads, the more nodes get vaccinated, making the e_B and k_B less accurate. Consider the real-world scenario that the epidemics control agency wants to identify the most influential disease spreaders and quarantine them. When the information spreads slowly, it is workable to identify the influential spreaders from the structure of contact network. But when information spreads fast, using only the contact data is not adequate any more. As for $\gamma^{\lambda}_{AB} > 3.0$, where the information spreads even faster, the value of τ becomes stable. This is because when the information spreads very fast, the number of vaccinated nodes achieves its upper limit, and the spreading influence of nodes impacted by the vaccination will not change. The change of other three parameters $\lambda_{AB}, \lambda_{BA}$ and m_s, does not influence the decreasing trend of τ, as demonstrated in Fig. 2(b)–(d).

Next, we work on the interlayer coupling strength. There are two parameters λ_{AB} and λ_{BA} reflecting the coupling strength between two layers. From Fig. 3(a), we can see that with the increase of λ_{AB}, τ_{k_B} decreases significantly, which implies that the simple degree centrality in layer B becomes worse to rank the node influence. As for τ_{e_B}, it first increases a little and then decreases. In general, τ decreases with the increase of λ_{AB}. This is because when λ_{AB} increases, the effect of layer A on B are getting stronger, thus the centrality on layer B are becoming less accurate under the asymmetrically interacting processes. Fig. 3(b) and (c) display similar trends as (a). In Fig. 3(d), it can be seen that with the increase of λ_{BA}, τ increases. When λ_{BA} is small, the amount of informed nodes in layer A caused by the notification from layer B is small. So the spreading of information relies more on the structure and centrality of nodes in layer A. In this case, the suppression of disease is more dependent on the structure of layer A, leading to the relatively low accuracy of centrality in layer B to predict the spreading influence of nodes. When λ_{BA} becomes large, more informed nodes in layer A are caused by the notification from their counterparts in layer B, so the the distribution of informed nodes is more random and the suppression of disease then depends less on the centrality of nodes in layer A. When the number of informed nodes is large enough, the distribution of them can be considered as uniform in layer A. In this case, the spreading influence of nodes in layer B are reduced proportionally to their degree. The larger λ_{BA} is, the stronger such effect is. Thus the τ increases as λ_{BA} increases. Fig. 3(e) and (f) display similar trends as (d). In real-world scenarios, if the infected individuals can timely report their heath status, corresponding to large λ_{BA}, then it is easier to identify correctly the influential disease spreaders. Otherwise, as the infected ones are hidden, it becomes more difficult to identify the influential spreaders under the interplay between information spreading and disease spreading. This will prevent effective epidemic control from the health agencies.

Finally, we discuss the effect of degree correlation m_s between layers. The spearman rank correlation coefficient is used to quantify the degree correlation of nodes in two layers. As shown in Fig. 4, the τ decreases with the increase of degree correlation m_s. Remember that at the initial step of interacting spreading, a seed node in layer B is infected and its counterpart in layer A is informed. The affected range of disease spreading from the seed node depends on the centralities of seed in both of layer A and B. From the aspect of degree correlation, all seeds can be divided into four cases: (1) nodes with large k_A and small k_B. In this case, because of their small degree in layer B, the spreading influence of such nodes is relatively small. Although the information spreading is large due to their large k_A, the suppression effect is less obvious. Thus the performance of centrality is not largely affected. (2) nodes with small k_A and large k_B. In this case, due to the centrality of seed, the range of

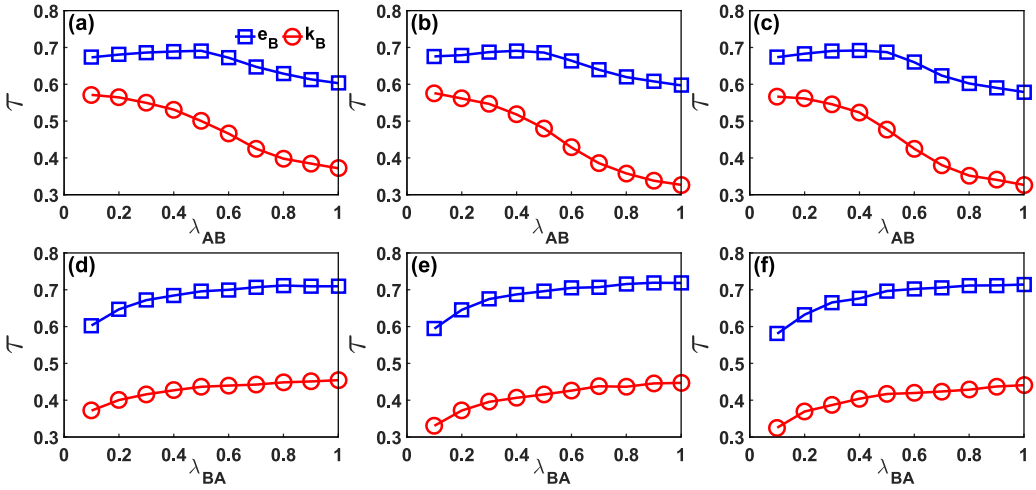

Fig. 3. Dependence of the Kendall's tau correlation of the eigenvector centrality and degree with the real spreading influence of nodes on the vaccination rate λ_{AB} (a)-(c) and informing rate λ_{BA} (d)-(e) respectively. When λ_{AB} increases, the τ_{e_B} first increases slightly and then decreases, while the τ_{k_B} keeps decreasing. When λ_{BA} increases, both τ_{e_B} and τ_{k_B} increase. Other parameters are set as (a) $\gamma^{\lambda}_{AB} = 2.0$, $m_s = 0.5$, $\lambda_{BA} = 0.1$, (b) $\gamma^{\lambda}_{AB} = 2.0$, $m_s = 0.7$, $\lambda_{BA} = 0.1$, (c) $\gamma^{\lambda}_{AB} = 2.4$, $m_s = 0.5$, $\lambda_{BA} = 0.1$,(d) $\gamma^{\lambda}_{AB} = 2.0$, $m_s = 0.5$, $\lambda_{AB} = 1.0$, (e) $\gamma^{\lambda}_{AB} = 2.0$, $m_s = 0.7$, $\lambda_{AB} = 1.0$ and (f) $\gamma^{\lambda}_{AB} = 2.4$, $m_s = 0.5$, $\lambda_{AB} = 1.0$.

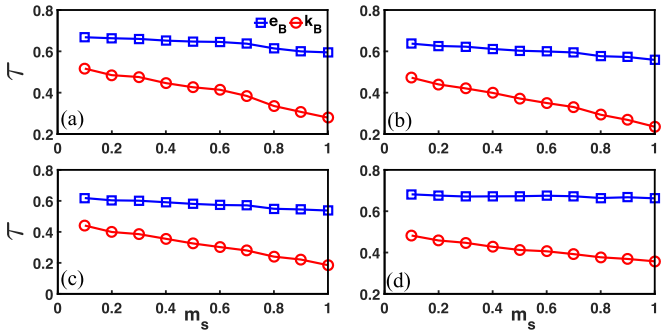

Fig. 4. Dependence of the Kendall's tau correlation of the eigenvector centrality and degree with the real spreading influence of nodes on the interlayer degree correlation m_s. Both τ_{e_B} and τ_{k_B} decrease as m_s increases. Other parameters are set as (a) $\gamma^{\lambda}_{AB} = 2.0$, $\lambda_{AB} = 0.7$, $\lambda_{BA} = 0.1$, (b) $\gamma^{\lambda}_{AB} = 2.0$, $\lambda_{AB} = 1.0$, $\lambda_{BA} = 0.1$, (c) $\gamma^{\lambda}_{AB} = 2.4$, $\lambda_{AB} = 1.0$, $\lambda_{BA} = 0.1$ and (d) $\gamma^{\lambda}_{AB} = 2.0$, $\lambda_{AB} = 1.0$, $\lambda_{BA} = 0.3$.

disease spreading is relatively large and the information spreading is small, thus there will be a small number of vaccinated nodes and the suppression effect is as well small. (3) nodes with large k_A and large k_B. For these nodes as initial spreaders in both layers, the suppression effect for disease spreading is obvious, making the centrality in predicting the disease spreading less accurate. The larger degree correlation m_s is, the more such kind of nodes are in the network, corresponding to the largely reduced τ in Fig. 4. (4) nodes with small k_A and small k_B. In this case, neither the disease nor information will break out and these nodes are ranked low in the list. In all, when the two-layer degree correlation is large, the suppression effect on the disease spreading is the largest, and the τ of centrality and spreading influence is impacted the most.

The above results imply that in real-world epidemic control where the information spreading and disease spreading interplay, using the contact network data is not adequate to accurately identify the critical spreaders, especially when the information spreads fast, the vaccination willingness of people is strong and the degree correlation is large. So to identify the influential spreaders more accurately in multiplex network, we need new framework and method which is our work in the next part.

V. Mapping to Bond Percolation

In this part, we map the coevolving spreading dynamics into bond percolation and calculate analytically the prevalence when the epidemic is originated from a single seed i in the multiplex network by using the message passage method. The message passing approach is an inference method that can provide exact predictions or good approximations analytically in many problems in network science, such as predicting the size of the giant component in percolation [46]. In the SIR dynamics, the ultimate outbreak size corresponds to the size of the giant component in percolation, which is of our interests.

We first introduce the percolation on a single network. In the percolation process, edges are occupied with probability T_p called transmissibility, and a giant component appears if T_p is sufficient high. The mapping of percolation to the SIR model is straight forward: edges are occupied with probability T_p, equal to the time-integrated probability T that infections occur on the edges. Here $T = 1 - e^{-\beta t}$ is the probability that a neighbor of an infected node is infected before it recovers, where β is the disease-causing infection probability and t is the time the infected node remains infective. If using the discrete time rather than continuous, which is common in computer simulation, then $T = 1 - (1 - \beta)^t$, where t is measured in time steps [47]. The giant component appearing in the percolation process corresponds to the potential epidemic outbreak of disease with a non-negligible fraction of the network size.

To map the coevolving dynamics on multiplex network into percolation process, we need the following assumption that the

information spreading is much faster than the epidemic spreading [48]. This is reasonable for the Internet times, as information is easily transmitted worldwide through online social media, telephone, mass media, et al. Like the COVID-19 epidemic, the whole world gets to know its information soon after its outbreak. In addition, the vaccination in layer B can be regarded as a type of "disease" because each node in layer B can be in either infected state or vaccinated state [42]. The disease spreading and vaccination are then viewed as two competing "diseases" on layer B. In the limit of large network size N, when two competing diseases spread, it can be considered as if they were spreading non-concurrently, one after the other [48]. So we can treat our coevolving dynamics as a fast dynamics of information spreading spreads first and a slow dynamics of disease spreading spreads subsequently.

A. Quenching the Fast Dynamics

First we consider the fast dynamics, i.e., the information spreading in layer A. This is a simple SIR process. Let $H^A_{i\to j}$ be the probability that node i is not connected to the giant component via node j. Then $H^A_{i\to j}$ can be obtained by the self-consistency equation [49]

$$H^A_{i\to j} = 1 - T^A + T^A \prod_{k\in\partial j\setminus i} H^A_{j\to k}, \tag{10}$$

where T^A is the edge occupation probability in percolation, and $\partial j \setminus i$ is the neighbor set of node j except i. This equation represents that either the edge connecting i and j is not occupied, or although it is occupied, j is not connected to the giant component through any of its neighbors other than i. The probability that i in the giant component is

$$P^A_i = 1 - \prod_{j\in\partial i} H^A_{i\to j}, \tag{11}$$

where ∂i is the neighbor set of node i. Mapping to SIR dynamics, $T^A = 1 - \mathrm{e}^{-\beta_A}$ when $t = 1$. $H^A_{i\to j}$ is the probability that node j by following the link from i does not trigger an outbreak with the transmissibility T^A. P^A_i is the probability that a node i in layer A triggers the epidemic outbreak in terms of $H^A_{i\to j}$.

B. Fast Dynamics as an Outer Field to Slow Dynamics

Now consider the slow dynamics in layer B. Let $H^B_{i\to j}$ be the probability that node i is not connected to the giant component via node j. This can happen because (a) the node j is vaccinated with probability $\lambda_{AB}P^A_i$; (b) the node j is not vaccinated, but the edge $i \to j$ is not occupied with probability $1 - \beta_B$; and (c) the node j is not vaccinated and the edge $i \to j$ is occupied, but node j is not connected to the giant component via any of its neighbors. Conclude the above scenarios we have

$$\begin{aligned} H^B_{i\to j} = {} & \lambda_{AB}P^A_i + \left(1 - \lambda_{AB}P^A_i\right)\left(1 - T^B\right) \\ & + T^B\left(1 - \lambda_{AB}P^A_i\right)\prod_{k\in\partial j\setminus i} H^B_{j\to k}, \end{aligned} \tag{12}$$

where $T^B = \beta_B$ because we simulate the SIR dynamics in discrete time and the infected nodes recover after one time step, corresponding to $t = 1$ in the above mentioned definition. The probability that i in the giant component is

$$P^B_i = 1 - \prod_{j\in\partial i} H^B_{i\to j}. \tag{13}$$

This P^B_i is the probability that a node i in layer B triggers an epidemic outbreak in terms of $H^B_{i\to j}$.

Then according to ref. [50], the size of epidemic when it originates from a seed i is

$$S^B_i = \frac{1}{N}\left(1 + \sum_{j=1, j\neq i}^{N} P^B_j\right). \tag{14}$$

As the seed i must be included in the epidemic outbreak, it corresponds to 1 in the summation. After obtaining the probability and the outbreak size, the average prevalence when the epidemic is initiated by a seed i is defined as

$$\rho^P_i = P^B_i * S^B_i. \tag{15}$$

Thus we can take ρ^P as the indicator of node influence in layer B in the asymmetrically interacting processes on multiplex network. The calculation of influence is described in algorithm 1.

Algorithm 1: Influence Calculation in Multiplex Network.

Input: the network of layer A G_A and layer B G_B; the information transmission rate λ_A, the disease transmission rate λ_B and the vaccination rate λ_{AB}

Output: the set of influence ρ^P_i of each node i as the initial seed

1: calculate $H^A_{i\to j}$ and P^A_i from network A
2: calculate $H^B_{i\to j}$ and P^B_i from network B
3: calculate S^B_i from network B
4: calculate ρ^P_i

VI. Evaluation of the Proposed Method in Identifying Influential Spreaders in Multiplex Network

Now we evaluate the effectiveness of the proposed method in identifying influential spreaders in multiplex network. As we have revealed that the dynamical interplay of the two layers impacts the spreading influence of nodes, we compare the accuracy of ρ^P with that of degree and eigenvector centrality as well as the state-of-the-art metrics of collective influence [9] and non-backtracking centrality [7] under different values of the parameters.

In Fig. 5, we vary the two-layer relative spreading rate γ^{λ}_{AB} and set all other parameters as fixed. It can be seen that the imprecision of the proposed metric ρ^P is much lower than that of the degree, eigenvector centrality and non-backtracking centrality. In general, ρ^P has a similar imprecision with CI_B, but when the fraction p of considered nodes is within 0.1, the ρ^P outperforms the CI_B in most cases.

Fig. 6 demonstrates the imprecisions of the considered metrics under different λ_{AB} and λ_{BA}. It can be seen in Fig. 6(a)–(c) that when λ_{AB} is within 0.5, our metric ρ^P is the best. As for

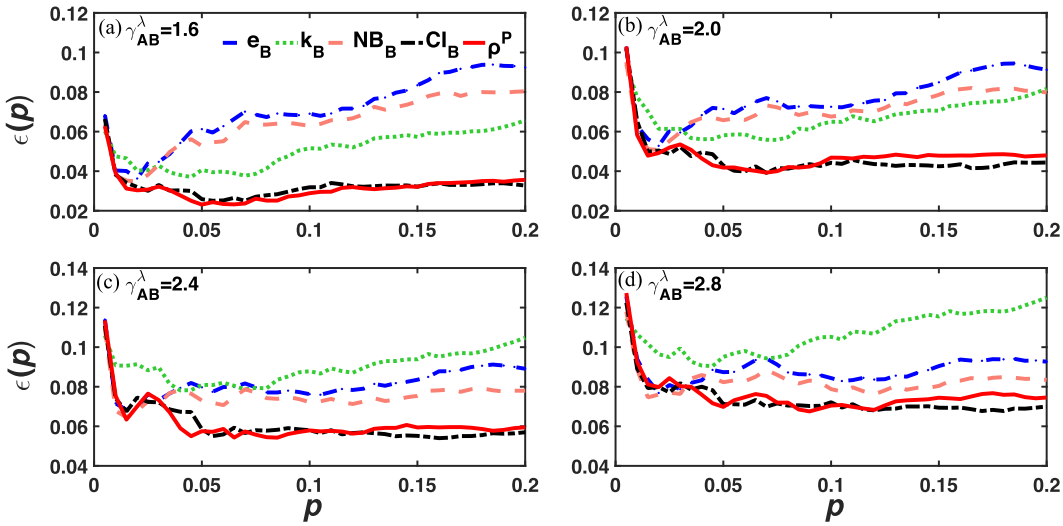

Fig. 5. The imprecisions of five metrics as a function of p under different γ^{λ}_{AB}. The imprecision of the proposed metric ρ^P is much smaller than that of eigenvector centrality, degree, non-backtracking centrality, while is close to that of collective influence. However, when $p \leq 0.1$, the ρ^P is the best indicator of influential spreaders. Other parameters are set as $\lambda_{AB} = 0.7$, $\lambda_{BA} = 0.1$, $m_s = 0.1$.

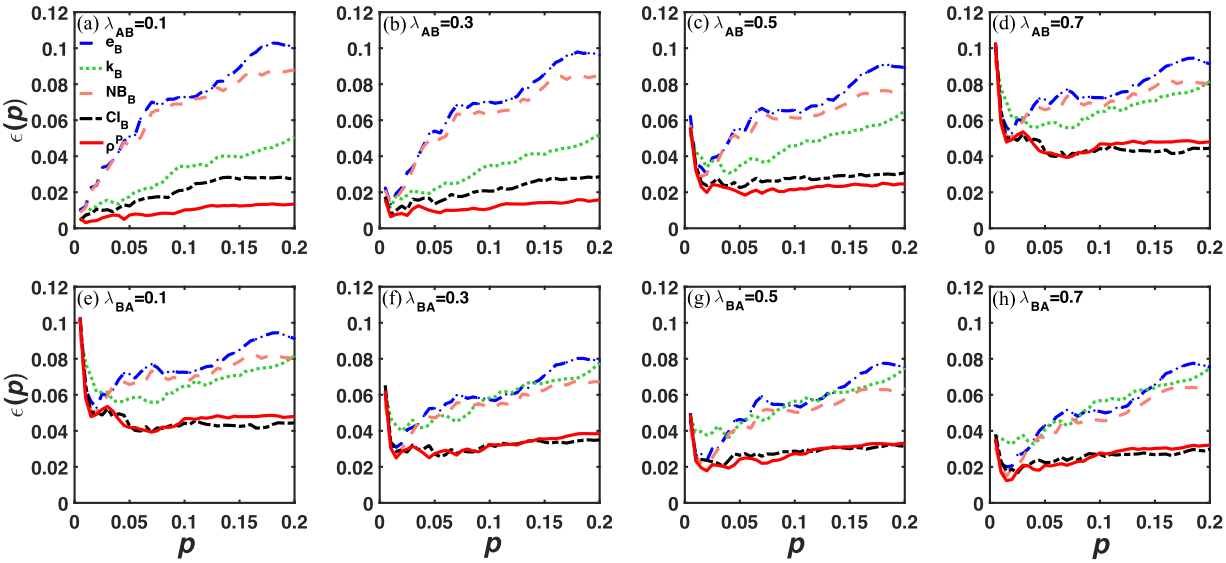

Fig. 6. The imprecisions of five metrics as a function of p under different λ_{AB} (a)-(d) and λ_{BA} (e)-(h). When λ_{AB} is within 0.5, imprecision of the proposed metric ρ^P is much smaller than that of eigenvector centrality, degree, non-backtracking centrality and collective influence. When $\lambda_{AB} = 0.7$, the imprecision of ρ^P is close to that of collective influence when $p \leq 0.1$. When λ_{BA} varies, the imprecision of ρ^P is much smaller than that of eigenvector centrality, degree, non-backtracking centrality, while is close to that of collective influence. However, when $p \leq 0.1$, ρ^P is the best indicator of influential spreaders. Other parameters are set as $\gamma^{\lambda}_{AB} = 2.0$, $m_s = 0.1$, $\lambda_{BA} = 0.1$ in (a)-(d), $\lambda_{AB} = 0.7$ in (e)-(h).

$\lambda_{AB} = 0.7$ in Fig. 6(d), the imprecision of ρ^P is much smaller than that of degree, eigenvector centrality and non-backtracking centrality and is very close to that of CI_B, but it becomes worse when $p \geq 0.1$. When the λ_{BA} varies, as shown in Fig. 6(e)–(h), the imprecision of ρ^P is significantly lower than that of k_B, e_B and NB_B in the considered range. The performance of ρ^P is close to or better than CI_B when $p \leq 0.1$, and becomes worse than CI_B when $p > 0.1$.

Fig. 7 demonstrates the imprecisions of the considered metrics under different values of degree correlation m_s. It can be seen that the performance of ρ^P is in general very close to CI_B. From Fig. 7(a) and (b) it can be seen that the imprecisions of both ρ^P and CI_B are better than that of degree, eigenvector centrality and non-backtracking centrality. When the degree correlation increases to 0.5 or 0.7, the imprecisions of ρ^P and CI_B are equal to or slightly higher than that of e_B and NB_B. We think this is because when we calculate the ρ^P, it is based on the assumption that the layer A spreads information first. When the degree correlation is large, the hub nodes in layer B are probably to be vaccinated. Then layer B is separated by the vaccinated nodes into several small clusters and a giant component. The calculation of ρ^P on layer B is less accurate because the network

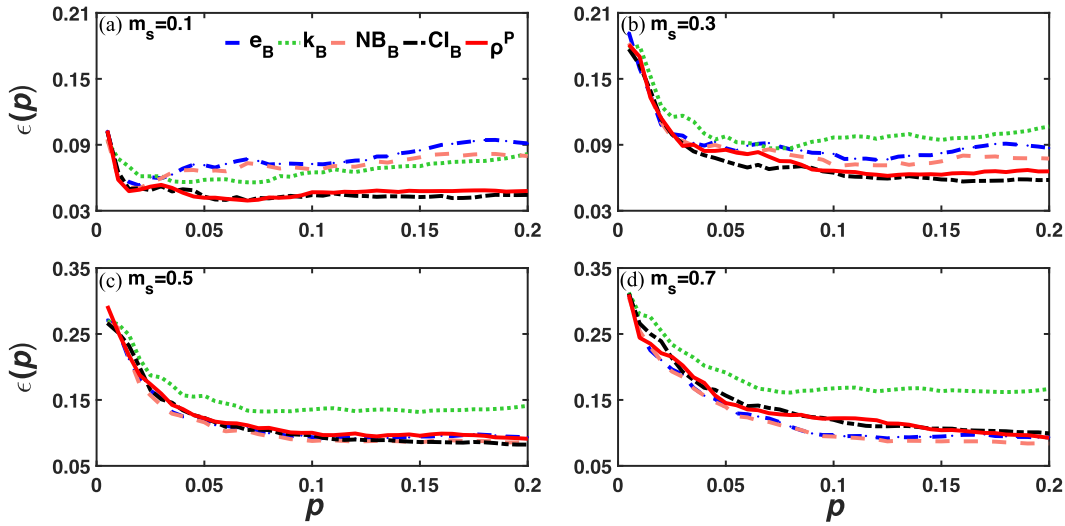

Fig. 7. The imprecisions of five metrics as a function of p under different degree correlation m_s. When $m_s = 0.1$, the imprecisions of ρ^P and CI_B are similar and smaller than that of e_B, k_B and NB_B. When m_s increases, the performance of ρ^P becomes worse. Other parameters are set as $\gamma^{\lambda}_{AB} = 2.0$, $\lambda_{AB} = 0.7$, $\lambda_{BA} = 0.1$.

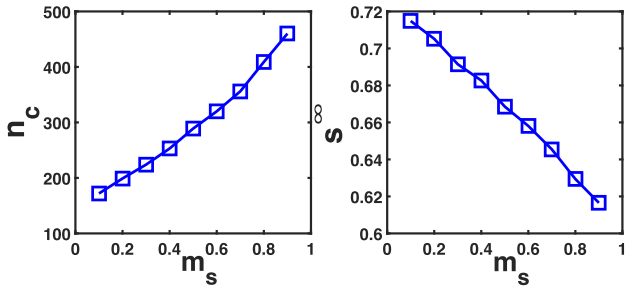

Fig. 8. Dependence of the number of components n_c and the size of giant component S^{∞} on degree correlation m_s. When m_s increases, the number of components in layer B increases and the size of giant component decreases, which means the network is broken. Other parameters are set as $\gamma^{\lambda}_{AB} = 2.0$, $\lambda_{AB} = 0.7$, $\lambda_{BA} = 0.1$.

has been dismantled. To evaluate this, we calculate the number of components and the size of giant component when m_s varies. As shown in Fig. 8, with the increase of degree correlation m_s, the number of components in layer B increases and the size of the giant component decreases.

Next we adjust the link overlap and degree-correlation of the two layers and compare the imprecisions of different metrics. The link overlap is the fraction of overlap edges in layer A and B, which positively relates to the degree correlation of the two layers. We set the degree correlation as 0.1 and 0.3, and adjust the link overlap respectively. As demonstrated in Fig. 9, the ρ^P is the best indicator to identify influential spreaders under the considered link overlap and degree correlations. The performance of collective influence CI_B is a bit worse than that of ρ^P. From the above results, we find that the ρ^P is a better metric than degree, eigenvector centrality and non-backtracking in the coevolving spreading dynamics. In many cases it is close to collective influence metric CI_B, but when identifying the most influential spreaders, i.e. $p \leq 0.1$, it exceeds the CI_B.

Finally, we examine the performance of the proposed metric on two real-world multiplex networks provided by [51], [52],

TABLE II
CHARACTERISTICS OF THE REAL-WORLD MULTIPLEX NETWORKS STUDIED IN THIS WORK

Network	N	E_A	E_B	m_s	λ_c^B	Type
SacchCere	4019	64100	59996	0.55	0.178	Biological
Pardus	2501	16119	20860	0.65	0.017	Social

These characteristics include the number of nodes N, the number of edges E_A in layer A and E_B in layer B, the interlayer degree correlation of the two layers m_s, the epidemic threshold λ_c^B in layer B, and the type of networks.

[53]. SacchCere is a biological network representing genetic interactions for organisms, and Pardus is a social network representing friendship relationship and message communication relationship between individuals in an online game virtual society 'Pardus(http://www.pardus.at). The properties of the two multiplex networks are displayed in Table II.

Fig. 10 demonstrates the results in two real-world multiplex networks and an adjusted Pardus network. In Fig. 10(a) and (d), it can be seen that in the SacchCere network, ρ^P is the best indicator to identify the most influential spreaders. While in Pardus social network as shown in Fig. 10(b) and (e), the imprecision of ρ^P is close to that of eigenvector centrality and non-backtracking centrality, but is obviously lower than that of the collective influence and degree. Since the degree correlation is an important factor that impacts the performance of ρ^P, we manually adjust down the degree correlation of the Pardus network to be $m_s = 0.1$ while keeping the degree sequence of each layer unchanged. As can be seen in Fig. 10(c) and (f) that the ρ^P becomes the best indicator of influential spreaders in the coevolving dynamics.

These results imply that in the modern world, where the spreading of information is very easy and fast worldwide, the centralities based on the contact layer alone may lose their effectiveness. To accurately identify the most influential spreaders and control the spread of epidemic disease, we need not only the physical contact network data, but also the information transmission network data and the coupling parameters.

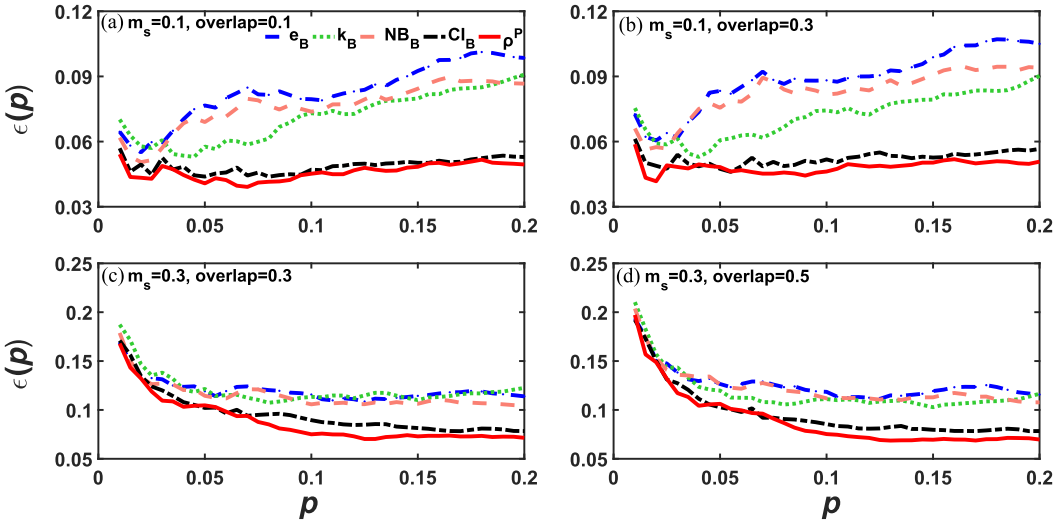

Fig. 9. The imprecision of five metrics as a function of p under different m_s and link overlap. The imprecision of ρ^P is the smallest and is obviously smaller than that of e_B, k_B and NB_B. Other parameters are set as $\gamma^{\lambda}_{AB} = 2.0$, $\lambda_{AB} = 0.7$, $\lambda_{BA} = 0.1$.

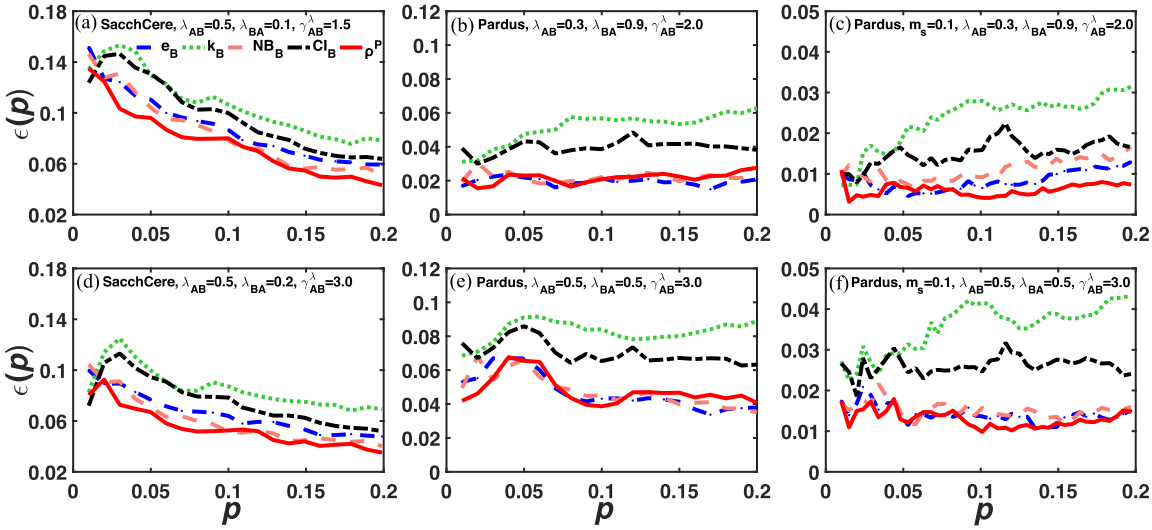

Fig. 10. The imprecisions of five metrics in two real-world multiplex networks. (a) and (d) Results on SacchCere network. The imprecision of ρ^P is the smallest among all considered metrics. (b) and (e) Results on Pardus network. The imprecision of ρ^P is obviously smaller than non-backtracking centrality and collective influence, while is close to that of eigenvector centrality and degree. (c) and (f) Results on adjusted Pardus network with the degree correlation being manually reduced to be 0.1. The imprecision of ρ^P is the smallest in most cases. In simulations, the disease transmission rate β_B is set as three times of epidemic threshold to ensure an outbreak.

VII. Conclusion

In this paper, we work on identification of influential spreaders in the multiplex networks. Firstly, we find out that the benchmark centralities like degree and eigenvector centrality in one layer alone can not predict the influential spreaders accurately due to the interplay between the spreading of information and disease on multiplex networks. The relative spreading rate of two layers, the interlayer dynamical coupling strength and the interlayer degree correlation play an important role in affecting the spreading influence of nodes. Then by mapping the coevolving spreading dynamics into bond percolation, we use the message-passing approach to calculate the epidemic outbreak size when spreading is initiated by a single seed. The obtained measure takes both the intralayer and interlayer structural and dynamical information into account and is thus very effective in identifying the most influential spreaders. Our work provides new ideas for making effective epidemic control strategy and gives a feasible framework to study the identification of critical nodes on multilayer networks. Although we study on the identification of critical nodes in the asymmetrically interacting spreading dynamics, the interacting dynamics on the multilayer network can be interdependent or competitive. How these interacting dynamics influence the functional importance of nodes is the question in future study.

The application of discovering the performance of centralities under different structural and dynamical parameters is meaningful in two aspects. On the one hand, due to the difficulty

in collecting network data, when we only have the contact layer data and calculate the centrality of nodes from the contact layer alone, we can evaluate how accurately the obtained centrality can predict the influential spreaders. On the other hand and more importantly, based on the network data of both layers, we should define new measure to accurately identify the most influential spreaders in the asymmetrically interacting dynamics. In the information-disease spreading model we use, the vaccination of an individual is very straightforward. But in reality, the vaccination behavior depends on many factors, such as attitudes of people, available resource and efficacy of the vaccine. If we take these factors into consideration, it generates new model which needs further study.

REFERENCES

[1] L. C. Freeman, "Centrality in social networks conceptual clarification," *Social Netw.*, vol. 1, no. 3, pp. 215–239, 1978.

[2] N. A. Christakis and J. H. Fowler, "Social contagion theory: Examining dynamic social networks and human behaviors," *Statist. Med.*, vol. 32, no. 4, pp. 556–577, 2013.

[3] F. Morone, G. D. Ferraro, and H. A. Makse, "The k-core as a predictor of structural collapse in mutualistic ecosystems," *Nature Phys.*, vol. 15, no. 1, pp. 95–102, 2019.

[4] L. C. Freeman, "A set of measures of centrality based upon betweenness," *Sociometry*, vol. 40, vol. 1, pp. 35–41, 1977.

[5] P. Bonacich and P. Lloyd, "Eigenvector-like measures of centrality for asymmetric relations," *Social Netw.*, vol. 23, no. 3, pp. 191–201, 2001.

[6] S. Brin and L. Page, "The anatomy of a large-scale hypertextual web search engine," *Comput. Netw.*, vol. 30, pp. 107–117, 1998.

[7] T. Martin, X. Zhang, and M. E. J. Newman, "Localization and centrality in networks," *Phys. Rev. E*, vol. 90, no. 5, 2014, Art. no. 052808.

[8] M. Kitsak et al., "Identification of influential spreaders in complex networks," *Nature Phys.*, vol. 6, no. 11, pp. 888–893, 2010.

[9] F. Morone and H. A. Makse, "Influence maximization in complex networks through optimal percolation," *Nature*, vol. 524, no. 7563, pp. 65–68, 2015.

[10] L. Lü et al., "The H-index of a network node and its relation to degree and corness," *Nature Commun.*, vol. 7, no. 1, 2016, Art. no. 10168.

[11] L. Zdeborová, P. Zhang, and H.-J. Zhou, "Fast and simple decycling and dismantling of networks," *Sci. Rep.*, vol. 6, 2016, Art. no. 37954.

[12] P. Clusella et al., "Immunization and targeted destruction of networks using explosive percolation," *Phys. Rev. Lett.*, vol. 117, no. 20, 2016, Art. no. 208301.

[13] Y. Liu et al., "Accurate ranking of influential spreaders in networks based on dynamically asymmetric link weights," *Phys. Rev. E*, vol. 96, no. 2, 2017, Art. no. 022323.

[14] S. Sen et al., "Influencer identification in dynamical complex systems," *J. Complex Netw.*, vol. 8, no. 2, 2020, Art. no. cnz029.

[15] M. Kivelä et al., "Multilayer networks," *J. Complex Netw.*, vol. 2, no. 3, pp. 203–271, 2014.

[16] A. Cardillo et al., "Modeling the multi-layer nature of the European air transport network: Resilience and passengers re-scheduling under random failures," *Eur. Phys. J. Special Topics*, vol. 215, no. 1, pp. 23–33, 2013.

[17] S. Boccaletti et al., "The structure and dynamics of multilayer networks," *Phys. Rep.*, vol. 544, no. 1, pp. 1–122, 2014.

[18] L. Chen, F. Ghanbarnejad, and D. Brockmann, "Fundamental properties of cooperative contagion processes," *New J. Phys.*, vol. 19, no. 10, 2017, Art. no. 103041.

[19] F. D. Sahneh and C. Scoglio, "Competitive epidemic spreading over arbitrary multilayer networks," *Phys. Rev. E*, vol. 89, no. 6, 2014, Art. no. 062817.

[20] R. Amato et al., "Opinion competition dynamics on multiplex networks," *New J. Phys.*, vol. 19, no. 12, 2017, Art. no. 123019.

[21] W. Wang et al., "Coevolution spreading in complex networks," *Phys. Rep.*, vol. 820, pp. 1–51, 2019.

[22] C. Granell, S. Gómez, and A. Arenas, "Dynamical interplay between awareness and epidemic spreading in multiplex networks," *Phys. Rev. Lett.*, vol. 111, no. 12, 2013, Art. no. 128701.

[23] C. Granell, S. Gómez, and A. Arenas, "Competing spreading processes on multiplex networks: Awareness and epidemics," *Phys. Rev. E*, vol. 90, no. 1, 2014, Art. no. 012808.

[24] S. Funk et al., "The spread of awareness and its impact on epidemic outbreaks," *Proc. Nat. Acad. Sci.*, vol. 106, no. 16, pp. 6872–6877, 2009.

[25] F. Battiston, V. Nicosia, and V. Latora, "Structural measures for multiplex networks," *Phys. Rev. E*, vol. 89, no. 3, 2014, Art. no. 032804.

[26] M. D. Domenico et al., "The physics of spreading processes in multilayer networks," *Nature Phys.*, vol. 12, no. 10, pp. 901–906, 2016.

[27] S. Osat, A. Faqeeh, and F. Radicchi, "Optimal percolation on multiplex networks," *Nature Commun.*, vol. 8, 2017, Art. no. 1540.

[28] G. J. Baxter, G. Timár, and J. F. F. Mendes, "Targeted damage to interdependent networks," *Phys. Rev. E*, vol. 98, no. 3, 2018, Art. no. 032307.

[29] A. Santoro and V. Nicosia, "Optimal percolation in correlated multilayer networks with overlap," *Phys. Rev. Res.*, vol. 2, no. 3, 2020, Art. no. 033122.

[30] D. Brockmann and D. Helbing, "The hidden geometry of complex, network-driven contagion phenomena," *Science*, vol. 342, no. 6164, pp. 1337–1342, 2013.

[31] A. Y. Lokhov and D. Saad, "Optimal deployment of resources for maximizing impact in spreading processes," *Proc. Nat. Acad. Sci.*, vol. 114, no. 39, pp. E8138–E8146, 2017.

[32] A. Halu et al., "Multiplex pagerank," *PLoS One*, vol. 8, no. 10, 2013, Art. no. e78293.

[33] J. Iacovacci et al., "Functional multiplex Pagerank," *Europhysics Lett.*, vol. 116, no. 2, 2016, Art. no. 28004.

[34] L. Solá et al., "Eigenvector centrality of nodes in multiplex networks," *Chaos: An Interdiscipl. J. Nonlinear Sci.*, vol. 23, no. 3, 2013, Art. no. 033131.

[35] D. Taylor, M. A. Porter, and P. J. Mucha, "Tunable eigenvector-based centralities for multiplex and temporal networks," *Multiscale Model. Simul.*, vol. 19, no. 1, pp. 113–147, 2021.

[36] M. D. Domenico et al., "Mathematical formulation of multilayer networks," *Phys. Rev. X*, vol. 3, no. 4, 2013, Art. no. 041022.

[37] D. Wang, H. Wang, and X. Zou, "Identifying key nodes in multilayer networks based on tensor decomposition," *Chaos: An Interdiscipl. J. Nonlinear Sci.*, vol. 27, no. 6, 2017, Art. no. 63108.

[38] M. D. Domenico et al., "Ranking in interconnected multilayer networks reveals versatile nodes," *Nature Commun.*, vol. 6, no. 1, 2015, Art. no. 6868.

[39] P. Basaras, G. Iosifidis, D. Katsaros, and L. Tassiulas, "Identifying influential spreaders in complex multilayer networks: A centrality perspective," *IEEE Trans. Netw. Sci. Eng.*, vol. 6, no. 1, pp. 31–45, Jan.–Mar. 2019.

[40] M. D. Domenico et al., "Centrality in interconnected multilayer networks," 2013, *arXiv1311.2906v1*.

[41] D. Zhao et al., "Identifying influential spreaders in interconnected networks," *Physica Scripta*, vol. 89, no. 1, 2013, Art. no. 015203.

[42] W. Wang et al., "Asymmetrically interacting spreading dynamics on complex layered networks," *Sci. Rep.*, vol. 4, no. 1, 2014, Art. no. 5097.

[43] Z. Ruan, M. Tang, and Z. Liu, "Epidemic spreading with information-driven vaccination," *Phys. Rev. E*, vol. 86, no. 3, 2012, Art. no. 036117.

[44] H. Yang et al., "Suppression of epidemic spreading in time-varying multiplex networks," *Appl. Math. Modelling*, vol. 75, pp. 806–818, 2019.

[45] M. G. Kendall, "A new measure of rank correlation," *Biometrika*, vol. 30, no. 1/2, pp. 81–93, 1938.

[46] A. Allard and L. Hébert-Dufresne, "On the accuracy of message-passing approaches to percolation in complex networks," 2019, *arXiv1906.10377v1*.

[47] M. E. J. Newman, "Spread of epidemic disease on networks," *Phys. Rev. E*, vol. 66, no. 1, 2002, Art. no. 016128.

[48] B. Karrer and M. E. J. Newman, "Competing epidemics on complex networks," *Phys. Rev. E*, vol. 84, no. 3, 2011, Art. no. 036106.

[49] B. Karrer, M. E. J. Newman, and L. Zdeborová, "Percolation on sparse networks," *Phys. Rev. Lett.*, vol. 113, no. 20, 2014, Art. no. 208702.

[50] B. Min, "Identifying an influential spreader from a single seed in complex networks via a message-passing approach," *Eur. Phys. J. B*, vol. 91, no. 1, 2018, Art. no. 18.

[51] C. Stark, B. -J. Breitkreutz, T. Reguly, L. Boucher, A. Breitkreutz, and M. Tyers, "BioGRID: A general repository for interaction datasets," *Nucleic Acids Res.*, vol. 34, no. 1, pp. D535–D539, 2006.

[52] M. De Domenico, V. Nicosia, A. Arenas, and V. Latora, "Structural reducibility of multilayer networks," *Nature Commun.*, vol. 6, 2015, Art. no. 6864.

[53] M. Szell, R. Lambiotte, and S. Thurner, "Multirelational organization of large-scale social networks in an online world," *Proc. Nat. Acad. Sci.*, vol. 107, no. 31, pp. 13636–13641, 2010.